# Fumarates improve psoriasis and multiple sclerosis by inducing type II dendritic cells

Kamran Ghoreschi,[1] Jürgen Brück,[1] Christina Kellerer,[1] Caishu Deng,[3,4] Haiyan Peng,[5] Oliver Rothfuss,[2] Rehana Z. Hussain,[3,4] Anne R. Gocke,[3,4] Annedore Respa,[1] Ivana Glocova,[1] Nadejda Valtcheva,[2] Eva Alexander,[2] Susanne Feil,[2] Robert Feil,[2] Klaus Schulze-Osthoff,[2] Rudolf A. Rupec,[6] Amy E. Lovett-Racke,[3,4,5] Ralf Dringen,[7] Michael K. Racke,[3,4,5] and Martin Röcken[1]

[1]Department of Dermatology, University Medical Center and [2]Interfaculty Institute for Biochemistry, Eberhard Karls University Tübingen, 72076 Tübingen, Germany
[3]Department of Neurology and Neurotherapeutics and [4]Center for Immunology, University of Texas Southwestern Medical Center, Dallas, TX 75390
[5]Department of Neurology, The Ohio State University Medical Center, Columbus, OH 43210
[6]Department of Dermatology and Allergology, Ludwig-Maximilians University Munich, 80337 Munich, Germany
[7]Center for Biomolecular Interactions Bremen, University of Bremen, 28359 Bremen, Germany

**Fumarates improve multiple sclerosis (MS) and psoriasis, two diseases in which both IL-12 and IL-23 promote pathogenic T helper (Th) cell differentiation. However, both diseases show opposing responses to most established therapies. First, we show in humans that fumarate treatment induces IL-4–producing Th2 cells in vivo and generates type II dendritic cells (DCs) that produce IL-10 instead of IL-12 and IL-23. In mice, fumarates also generate type II DCs that induce IL-4–producing Th2 cells in vitro and in vivo and protect mice from experimental autoimmune encephalomyelitis. Type II DCs result from fumarate-induced glutathione (GSH) depletion, followed by increased hemoxygenase-1 (HO-1) expression and impaired STAT1 phosphorylation. Induced HO-1 is cleaved, whereupon the N-terminal fragment of HO-1 translocates into the nucleus and interacts with AP-1 and NF-κB sites of the IL-23p19 promoter. This interaction prevents IL-23p19 transcription without affecting IL-12p35, whereas STAT1 inactivation prevents IL-12p35 transcription without affecting IL-23p19. As a consequence, GSH depletion by small molecules such as fumarates induces type II DCs in mice and in humans that ameliorate inflammatory autoimmune diseases. This therapeutic approach improves Th1- and Th17-mediated autoimmune diseases such as psoriasis and MS by interfering with IL-12 and IL-23 production.**

CORRESPONDENCE
Martin Röcken:
mrocken@med.uni-tuebingen.de
OR
Michael K. Racke:
Michael.Racke@osumc.edu

Abbreviations used: BMDC, BM-derived DC; ChIP, chromatin immunoprecipitation; DMF, dimethylfumarate; EAE, experimental autoimmune encephalomyelitis; GSH, glutathione; H3Ac, histone 3 acetylation; IBD, inflammatory bowel disease; MBP, myelin basic protein; MMF, monomethylfumarate; mRNA, messenger RNA; MS, multiple sclerosis; NAC, N-acetylcysteine; ROS, reactive oxygen species; RT-PCR, real-time PCR; siRNA, small interfering RNA.

Inflammatory autoimmune diseases such as multiple sclerosis (MS), inflammatory bowel disease (IBD), and psoriasis are a major health burden especially in industrialized countries, affecting up to 5% of the population. Genetic analyses, functional data, and experimental animal studies showed that these diseases have aberrant induction of IL-12–producing DCs and IFN-γ^{+} Th1 cells as well as IL-23–producing DCs and IL-17^{+} Th17 cells, whereas IL-4 is virtually absent (Frohman et al., 2006; Burton et al., 2007; Nair et al., 2009; Nestle et al., 2009). Despite these insights, treatment of inflammatory autoimmune diseases remains challenging, and their differential

response to novel therapies is largely unexplained. Relapsing MS is attenuated by IFN-β (Frohman et al., 2006; Axtell et al., 2010) or inhibitors of T cell migration (Polman et al., 2006), whereas anti–IL-12/IL-23p40 mAb did not improve MS (Segal et al., 2008). In contrast, anti–IL-12/IL-23p40 mAb improves psoriasis and psoriatic arthritis (Krueger et al., 2007). Similarly, TNF inhibitors improve psoriasis, psoriatic arthritis, and IBD, whereas they exacerbate MS (Frohman et al., 2006; Kneilling et al., 2009). Thus, even though MS, psoriasis, and IBD as

autoimmune diseases share some immunological similarities, a common therapeutic agent is still lacking.

Dimethylfumarate (DMF) is a small molecule that is approved as a combination with the structurally related monomethylfumarate (MMF) for the treatment of psoriasis in some countries. Prospective phase II trials demonstrated that treatment with DMF is effective in both psoriasis (Altmeyer et al., 1994; Ghoreschi et al., 2003a) and MS (Kappos et al., 2008). Consequently, DMF is one of the first small molecules that directly improve the two autoimmune diseases, psoriasis and MS, which are both associated with pathogenic Th1 and Th17 cells; yet the mechanisms underlying the therapeutic efficacy remain undefined.

Some studies have implicated fumarates in DCs and Th cell survival or differentiation (de Jong et al., 1996; Litjens et al., 2004); others suggest a mode of action that is not related to immunity (Loewe et al., 2002; Kappos et al., 2008). No data exist on direct ex vivo analysis of DCs or T cells from either mice or humans treated with fumarates; data from a small number of psoriasis patients treated with a DMF/MMF-containing formulation suggest that fumarates favor Th2 development, yet the data did not provide a definitive conclusion (Litjens et al., 2003). The exact mechanisms leading to the improvement of MS remain unexplained (Kappos et al., 2008). Structurally, DMF is an $\alpha,\beta$-unsaturated carboxylic acid ester that binds glutathione (GSH), the cell's most important scavenger of reactive oxygen species (ROS). Thus, despite conflicting data (Mrowietz and Asadullah, 2005), DMF depletes intracellular stores of GSH most likely by conjugate formation. This is interesting in the context of genetic linkage analyses that correlated the risk of high IgE and ROS-aggravated type I allergy to distinct GST (GSH S-transferase) genotypes (Gilliland et al., 2004). As a consequence, GSH metabolism may affect the capacity to cope with oxidative stress and as a result control the development of either Th1 or Th2 responses (Jeannin et al., 1995; Gilliland et al., 2004). This explanation is in agreement with independent data correlating intracellular ROS concentrations with IL-12 production by DCs (Peterson et al., 1998). The therapeutic success of fumarates in psoriasis and MS on one side and the potential immune modulation caused by oxidative stress on the other may both result from the depletion of GSH, the common target molecule of fumarates.

To test this hypothesis, we analyzed the effects of fumarates on human and mouse immune responses in vitro and in vivo, focusing on DCs and their impact on Th cell differentiation. DMF treatment of DCs diminished intracellular GSH stores by 50%, increased hemoxygenase-1 (HO-1) levels, and inhibited phosphorylation of STAT1 in activated DCs. Surprisingly, STAT1 activation and, downstream, IFN consensus sequence-binding protein (ICSBP/IRF-8) signaling was required for IL-12p35 transcription but not for IL-23p19. In contrast, induction of HO-1 impaired IL-23p19 expression, without affecting IL-12p35. As a consequence, GSH depletion generated type II DCs (Menges et al., 2002; Schuler et al., 2003; Mazzoni and Segal, 2004; Dudziak et al., 2007)

that produced IL-10 instead of IL-12 and IL-23. The generation of type II DCs by fumarates induced GATA3-expressing Th2 cells, in vitro and in vivo, and protected mice from developing experimental autoimmune encephalomyelitis (EAE).

## RESULTS

### Fumarate therapy induces IL-4–producing CD4+ T cells in humans

Clinical trials demonstrated the efficacy of DMF therapy in MS (Kappos et al., 2008) and psoriasis (Altmeyer et al., 1994). To study the effects of DMF therapy on human
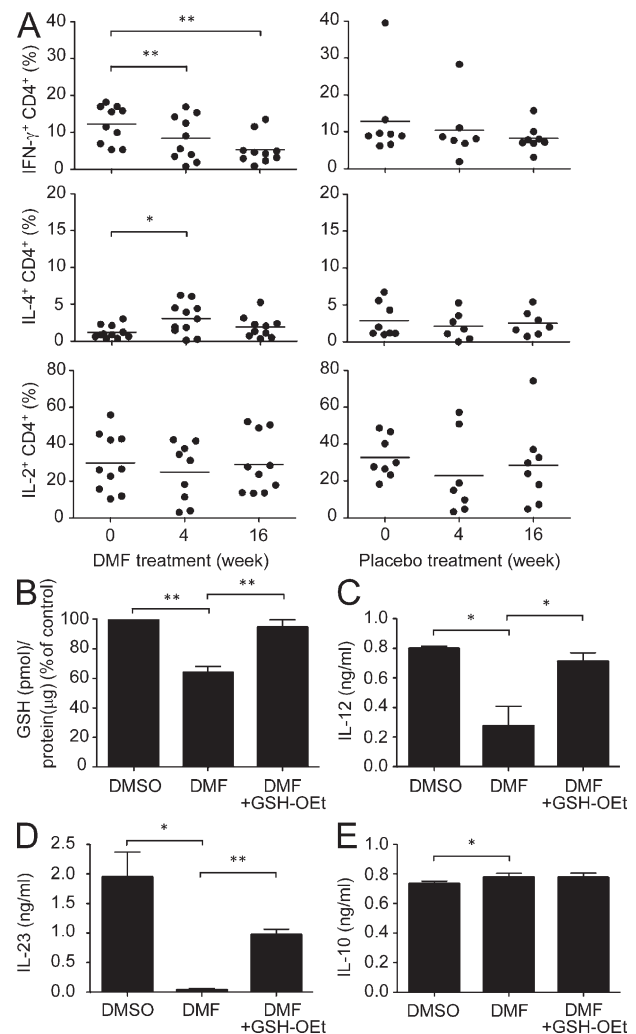


**Figure 1.** **DMF therapy induces Th2 responses in human CD4+ T cells in vivo and human type II DCs.** (A) CD4+ T were isolated from patients with psoriasis treated with either DMF or placebo at the indicated time of therapy and treated with PMA and ionomycin. IL-2, IL-4, and IFN-γ were assessed by intracellular flow cytometry. Each data point represents an individual patient sample (*, P < 0.05; **, P < 0.01). Horizontal bars represent the mean. (B) Quantification of intracellular GSH content of DCs treated with DMSO, 70 µM DMF, or 70 µM DMF and 1 mM GSH-OEt. Results are pooled data from four human donors (mean ± SEM; **, P < 0.01). (C–E) Human DCs were incubated with DMSO, 70 µM DMF, or DMF + 1 mM GSH-OEt and then treated with LPS for 18 h. IL-12, IL-23, or IL-10 production was determined by ELISA. Data were pooled from three donors (mean ± SEM; *, P < 0.05; **, P < 0.01).

immune responses, we analyzed the intracellular cytokine production of freshly isolated CD4$^+$ and CD8$^+$ T cells from 19 patients enrolled in a double-blind, placebo-controlled trial after 0, 4, and 16 wk of DMF treatment for psoriasis. In the DMF-treated group, the percentage of IFN-$\gamma^+$CD4$^+$ T cells decreased significantly over the entire study period, whereas the percentage of IL-4$^+$CD4$^+$ T cells peaked at 4 wk (Fig. 1 A). This increase of IL-4$^+$CD4$^+$ T cells was transient, but the ratio of IL-4/IFN-$\gamma^+$ CD4$^+$ T cells significantly increased at 4 wk as well as 16 wk of treatment (P < 0.05; not depicted). DMF therapy did not affect the percentage of IL-2$^+$CD4$^+$ T cells (Fig. 1 A) or the cytokine pattern of CD8$^+$ T cells (not depicted). In contrast, in the placebo group, the percentage of IL-4$^+$CD4$^+$ and IFN-$\gamma^+$CD4$^+$ T cells (Fig. 1 A) as well as the ratio of both populations (not depicted) remained stable over time, showing that the cytokine changes were specific for CD4$^+$ T cells in DMF-treated patients. Consistent with data from previous studies, fumarate-mediated inhibition of Th1 cells and the induction of Th2 cells correlated with the clinical improvement of psoriasis (not depicted; Ghoreschi et al., 2003a,b; Litjens et al., 2003).

## Fumarate–mediated induction of human type II DCs

As DMF forms conjugates with GSH, DMF should diminish intracellular GSH levels. Because of the conflicting published data (Mrowietz and Asadullah, 2005), we first determined the effects of DMF on GSH levels in human DCs and macrophages. Therapeutic DMF concentrations depleted intracellular GSH by 50%; GSH levels were fully restored by the cell-permeable ROS scavenger GSH-OEt (GSH reduced ethyl ester; Fig. 1 B). Simultaneously, DMF impaired the capacity of DCs or macrophages to produce either IL-12 (Fig. 1 C) or IL-23 (Fig. 1 D) in response to the TLR4 ligand LPS. In contrast, their capacity to produce IL-10 was slightly, but significantly increased (P < 0.05; Fig. 1 E). Thus, DMF may promote type II DCs. In contrast to the effects of fumarates on DCs, fumarates had no detectable effect on purified T cells (not depicted).

## Fumarate–mediated induction of mouse type II macrophages and type II DCs

To precisely analyze the effects of DMF in vitro and in vivo, we investigated the role of DMF in mice. We analyzed DMF-mediated GSH depletion in DCs, macrophages, and T cells of mice and in an animal model of Th1- and Th17-mediated disease, EAE. DMF depleted GSH in BM-derived DCs (BMDCs) of mice to the same extent as in human DCs (Fig. 2 A). As observed for human DCs, DMF treatment impaired IL-12 and IL-23 production by ≥90%, while significantly increasing IL-10 production by mouse DCs (Fig. 2 B). We postulated that DMF-mediated modulation of cytokine production might be regulated by ROS. We fully restored intracellular GSH levels of DMF-treated macrophages or DCs with either GSH-OEt or $N$-acetylcysteine (NAC; Fig. 2 C). Replenishing intracellular GSH partially restored the capability of DCs to make IL-12 or IL-23 (Fig. 2 B). The effects were similar to those obtained with human macrophages and DCs (Fig. 1, B–E). To ask whether DMF affects cytokine production through induction of ROS, we directly exposed DCs to $H_2O_2$ and stimulated the cells with LPS. $H_2O_2$ mirrored the DMF-dependent modulation of IL-12, IL-23, or IL-10 production (not depicted). Depletion of the ROS scavenger GSH with either $H_2O_2$ or with DMF had identical effects on DC cytokine production; importantly, both were fully reversed by GSH-OEt or NAC, directly demonstrating the key role of GSH in the modulation of DC function by DMF. Similar results were obtained with a second GSH-depleting fumarate, MMF (not depicted).

## ROS–mediated inhibition of either IL–12 or IL–23 through distinct signaling pathways

ROS may directly regulate various signaling pathways, including p38, Nrf2, or HO-1. In agreement with other experimental conditions (Durchdewald et al., 2007), we found no major effect of ROS-mediated GSH depletion on LPS-induced Nrf2 messenger RNA (mRNA) expression (not depicted). In contrast, quantitative real-time PCR (RT-PCR) revealed that DMF increased HO-1 expression in LPS-activated
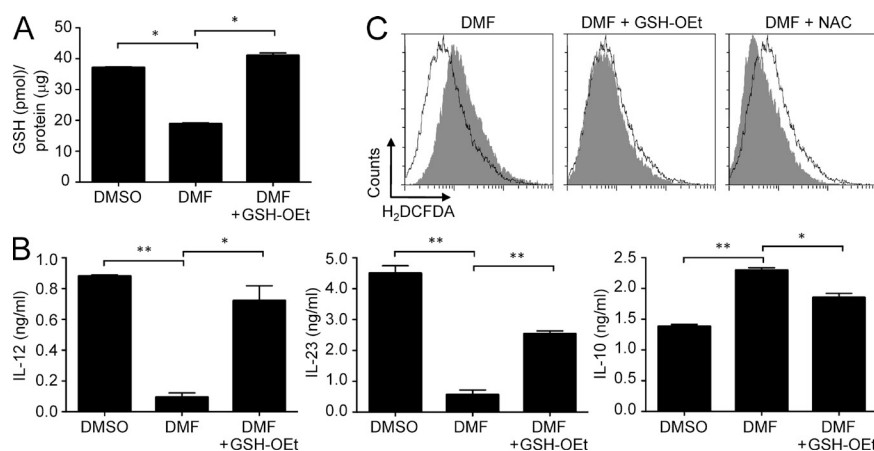


**Figure 2. DMF induces mouse type II macrophages and type II DCs.** (A) BMDCs were incubated with DMSO, 70 µM DMF, or DMF + 1 mM GSH-OEt, and GSH content was determined by a colorimetric assay (mean ± SEM; *, P < 0.001). (B) DCs were treated with DMSO, 70 µM DMF, or DMF + 1 mM GSH-OEt and then stimulated with LPS for 18 h. Culture supernatants were harvested, and the indicated cytokines were determined by ELISA (mean ± SEM; *, P < 0.01; **, P < 0.001). (C) DCs were incubated with DMSO, 70 µM DMF, DMF + 1 mM GSH-OEt, or DMF and 1 mM NAC for 2–4 h, and intracellular ROS levels were assessed by staining with 2',7'dichlorofluorescein. Intracellular ROS, gray; DMSO-treated controls, open. One representative experiment of three is shown.

DCs (Fig. 3 A). As HO-1 is a ROS-sensitive heat shock protein (Keyse and Tyrrell, 1989), we determined the impact of HO-1 induction on either IL-12 or IL-23 production. To address this point, we transfected DCs with HO-1 small interfering RNA (siRNA) before DMF treatment and LPS stimulation. HO-1 siRNA simultaneously prevented LPS-mediated induction of HO-1 in DMF-treated DCs and restored IL-23p19 mRNA expression by DMF-treated DCs (Fig. 3, A and B). Moreover, it partly restored IL-12/IL-23p40 mRNA transcription (Fig. 3 B) and, as a consequence, IL-23 protein production. In sharp contrast, HO-1 siRNA had no effect on the expression of IL-12p35 mRNA (Fig. 3 B), and IL-12 production remained undetectable. To confirm
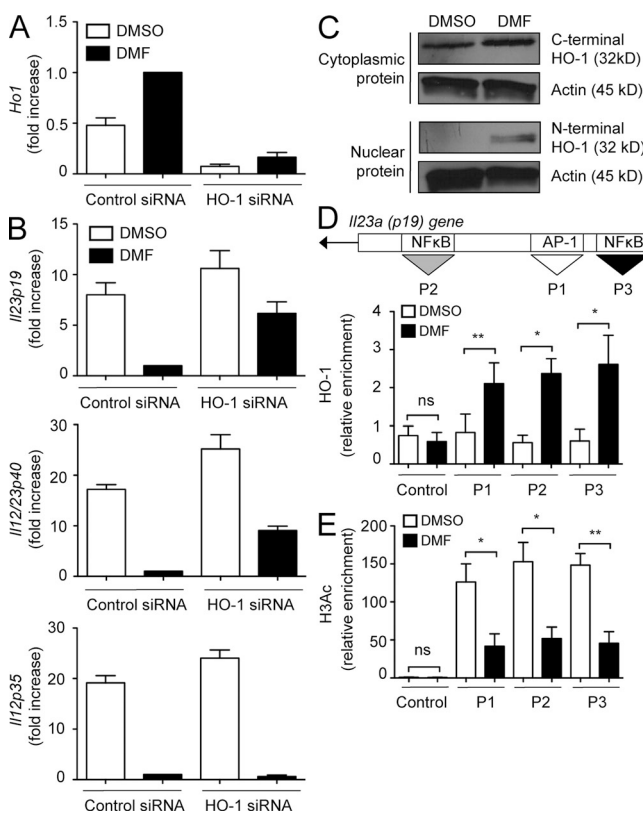
that HO-1 suppresses IL-23p19 without affecting IL-12p35, we used HO-1 (Ad–HO-1–EGFP) or control (Ad-EGFP) adenovirus for overexpression of this ROS-sensitive heat shock protein in DCs. Infection with HO-1 adenovirus prevented LPS-induced expression of IL-23p19 mRNA, whereas LPS-induced expression of IL-12p35 mRNA was not affected (Fig. S1, A and B). This pronounced effect of HO-1 on IL-23 was surprising, as HO-1 has not been described as a classical transcription factor. Yet, truncated HO-1 lacking a C-terminal part has been demonstrated to migrate into the nucleus during ROS stress, where it directly modulates the activity of transcription factors such as AP-1 or NF-κB (Lin et al., 2007). We confirmed nuclear translocation of the N-terminal truncated HO-1 protein in response to DMF-induced ROS stress, whereas the C-terminal part remained in the cytoplasm (Fig. 3 C).

Next we analyzed whether DMF-induced HO-1 associates with putative AP-1 and/or NF-κB sites that control the IL-23p19 promoter (Carmody et al., 2007; Mise-Omata et al., 2007; Liu et al., 2009). For that purpose, we performed chromatin immunoprecipitation (ChIP) assays using anti–HO-1 antibody. Indeed, we detected specific enrichment of three defined regions of the IL-23 promoter in DMF-treated DCs but not in control DCs (Fig. 3 D). These regions contain binding sites for either AP-1 or NF-κB (RelA and c-Rel). We next explored the effect of HO-1 binding on
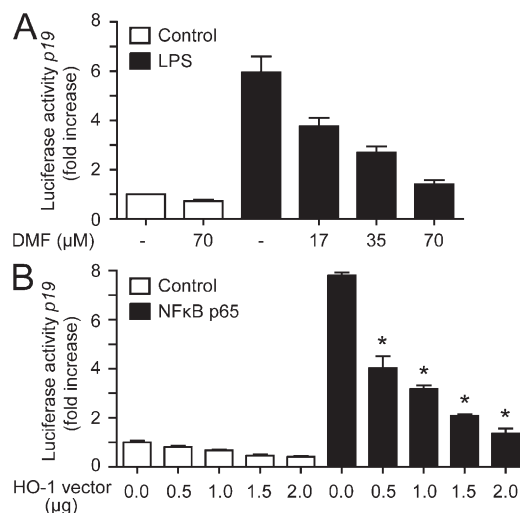


Figure 3.  **DMF–induced HO-1 selectively prevents IL-23 induction.** (A) DCs were treated with DMSO or 70 µM DMF, and HO-1 mRNA expression was determined by quantitative RT-PCR. HO-1 data were normalized to β-actin, and HO-1 level in control siRNA–transfected DMF–treated DCs was set as 1.0. The results are representative of three independent experiments. Error bars represent SEM. (B) HO-1 was knocked down, and levels of IL-12/IL-23p40, IL-23p19, or IL-12p35 mRNA were determined by RT-PCR. Data (mean ± SEM) were normalized to β-actin, and message levels in control siRNA–transfected DMF-treated DCs were set as 1.0. (C) DCs were treated as in A and lysed, and nuclear or cytoplasmic cell extracts were analyzed by Western blotting using antibodies directed against C- or N-terminal HO-1 protein. (D and E) DCs treated as in A were activated with LPS, cross-linked, and immunoprecipitated with anti–HO-1 (D) or anti-H3Ac (E). Bound DNA was amplified by quantitative PCR for primer sites P1 (AP-1; position 412–422 bp), P2 (c-Rel; position 560–584 bp), and P3 (RelA/c-Rel; position 394–406 bp). Data were pooled from four separate experiments and represent mean ± SEM (*, P < 0.05; **, P < 0.01; ns, not significant).



Figure 4.  **Interaction of DMF–induced HO-1 with the NF–κB p65–binding site directly inhibits IL-23p19 promoter activity.** (A) RAW246.7 cells were transfected with a reporter construct containing the IL-23p19 promoter and treated with the indicated doses of DMF. Luciferase activity was measured after stimulation with 100 ng/ml LPS for 6 h. Data from one representative of two independent experiments are shown. Error bars represent SEM. (B) NIH 3T3 cells were transfected with a reporter construct containing the IL-23p19 promoter (1 µg/well) alone or together with the expression vector for p65 (1 µg/well), as well as the HO-1 or the empty control vector at the indicated concentration. Pooled data from two separate experiments with duplicates are shown (mean ± SEM; *, P < 0.001 relative to the empty vector control). Reporter gene data were normalized to the activity of cotransfected β-galactosidase.

histone 3 acetylation (H3Ac) status, which is a characteristic positively associated with transcriptional activation. The data show that enrichment for HO-1 was associated with a significant reduction in H3Ac modification of the IL-23p19 promoter (Fig. 3 E). As nuclear HO-1 interferes with the transcriptional activity of AP-1 or NF-κB (Lin et al., 2007), our data show that HO-1 interaction most likely negatively modulates the transcriptional activity of AP-1 and NF-κB on the IL-23p19 promoter in DCs. To test whether this interaction was functional, we transfected macrophages with an IL-23p19 luciferase promoter construct. Treatment of these cells with DMF led to a dose-dependent inhibition of the LPS-induced IL-23p19 promoter activity (Fig. 4 A). To further analyze whether the interaction of HO-1 with NF-κB p65 directly affects the IL-23p19 promoter, we transfected fibroblasts with an IL-23p19 promoter reporter plasmid and vectors that contain p65, HO-1, or empty control vector. As expected, p65 induced strong reporter activity of the IL-23p19 promoter. Importantly, HO-1 but not the empty vector dose-dependently inhibited the IL-23p19 promoter activity (Fig. 4 B). Together, the data show that fumarate-induced HO-1 directly impairs IL-23p19 transcription.

Because HO-1 induction has been observed together with impaired STAT1 activation in MHC class II+ cells (Chora et al., 2007), we asked whether DMF diminishes IL-12p70 expression through STAT1 signaling. We found that DMF inhibited STAT1 phosphorylation (p-STAT1) in activated DCs without affecting p38 phosphorylation (Fig. 5 A). Activated STAT1 directly induces ICSBP/IRF-8, a transcription

factor binding to promoter elements of IL-12/IL-23p40 (Zhu et al., 2003) and IL-12p35 (Liu et al., 2004). We therefore examined the downstream effects of p-STAT1 on IL-12 and IL-23 induction in DCs. First, DMF prevented LPS-mediated induction of ICSBP (at 4 h; Fig. 5 B) and later of IL-12p70 expression (Fig. 5 C). The effects resulted from DMF-induced oxidative stress, as addition of GSH-OEt fully restored the p-STAT1 signaling cascade (Fig. 5 A), including expression and production of IL-12 (Fig. 2 B). To determine the requirement of p-STAT1 for IL-12p70 and IL-23 production, we stimulated STAT1−/− DCs with LPS. In agreement with published data (Gautier et al., 2005), IL-12 production was suppressed in activated STAT1−/− DCs compared with STAT1+/+ DCs (Fig. 5 D). In sharp contrast, IL-23 production and IL-10 production were unaffected in STAT1−/− DCs (Fig. 5 D), demonstrating that the p-STAT1–ICSBP signaling cascade was mainly required for IL-12 production (Zhu et al., 2003; Liu et al., 2004; Gautier et al., 2005). Consequently, GSH depletion by fumarates affected IL-12 and IL-23 production by interfering with two distinct signaling pathways, a finding that may explain why STAT1−/− mice remain fully sensitive to IL-23–dependent EAE (Bettelli et al., 2004).

To directly determine whether DMF also affected DC function in vivo, we treated mice with DMF at doses equivalent to those used in humans, isolated CD11c+ DCs by positive sorting from lymph nodes, and stimulated these DCs with LPS for cytokine expression and production. Quantitative RT-PCR showed that in vivo treatment with DMF affected DC function exactly as it did in vitro. DMF treatment in vivo increased HO-1 expression (Fig. 6 A) and impaired IL-12/IL-23p40 mRNA expression and IL-12 protein expression by DCs (Fig. 6, B and C). Thus, GSH depletion and ROS induction by DMF inhibited IL-12 and IL-23 production by interfering with two distinct signaling pathways:
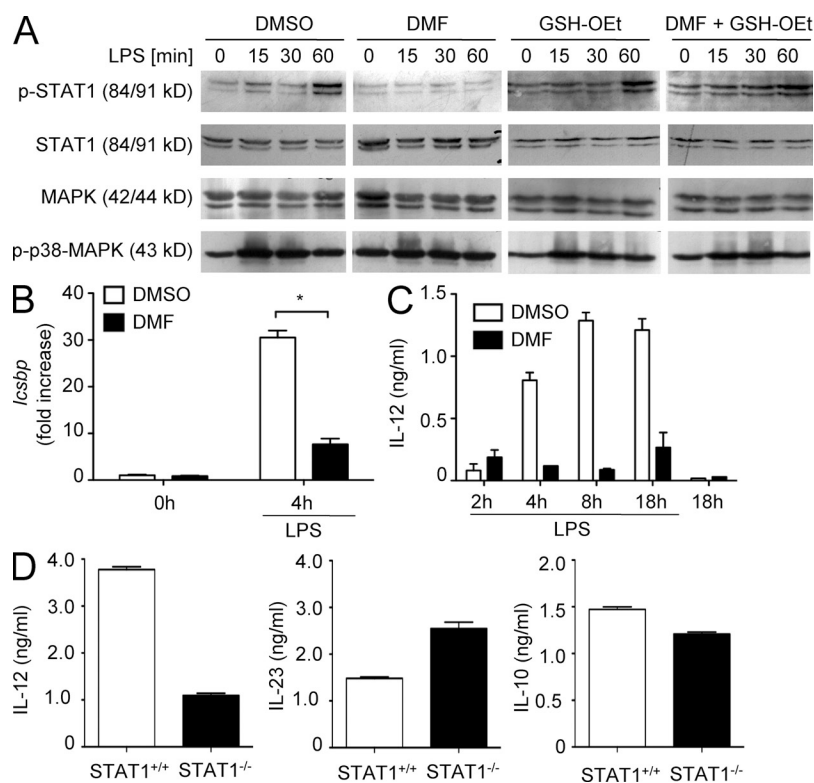


Figure 5. DMF treatment selectively impairs IL-12 induction through inhibition of the p-STAT1–ICSBP–IL-12 signaling pathway. (A) DCs were treated with DMSO, 70 μM DMF, 1 mM GSH-OEt, or DMF + GSH-OEt and stimulated for the indicated time with LPS. STAT1, p-STAT1, MAPK, and p-p38 MAPK content of cell lysates was analyzed by Western blot. (B) DCs were incubated with DMSO or DMF and activated with LPS for 4 h. ICSBP expression was assessed by RT-PCR, and data were normalized to β-actin and expressed as fold increase (mean ± SEM; *, P < 0.01). ICSBP level in unstimulated cells (0 h) was set as 1.0. (C) DCs were incubated with DMSO or 70 μM DMF and stimulated with LPS for the indicated times. IL-12 levels in the culture supernatants were analyzed by ELISA. Error bars represent SEM. (D) DCs from STAT1+/+ or STAT1−/− mice were stimulated for 18 h with LPS. The indicated cytokines in culture supernatants were analyzed by ELISA. Data from one out of four experiments with similar results are shown (mean ± SEM).

IL-12p35 expression required STAT1 phosphorylation, whereas it was independent of HO-1 induction. In sharp contrast, ROS-mediated induction of HO-1 suppressed IL-23p19 mRNA, and in part IL-12/IL-23p40, as demonstrated by HO-1 siRNA. This negative regulation of IL-12 and IL-23 was shown across several mouse strains (Fig. S2, A and B) and for human DCs from multiple donors (Fig. 1, C–E).

## Fumarates induce functional type II DCs that promote Th2 cell differentiation in vitro

These pronounced effects of fumarates on the production of IL-12, IL-23, and IL-10 should affect the capacity of DCs to prime CD4+ T cells for differentiation into Th1/Th17 cells or into Th2 cells (Biedermann et al., 2001b; Napolitani et al., 2005). To test this hypothesis, we stimulated DMF- or DMSO-treated DCs with LPS and analyzed their capacity to influence the differentiation of naive or in vivo primed CD4+ T cells into Th1, Th17, or Th2 cells. We first stimulated naive, TCR transgenic CD4+ T cells with OVA peptide and DCs, either in the presence or absence of DMF or MMF, which is a DMF derivative with comparable effects on DCs (not depicted). We first quantified transcription factors that determine T cell differentiation. In the absence of DMF, DCs induced CD4+ T cells expressing T-bet and ROR-γt mRNA and protein, the transcription factors which determine



A

B

C

**Figure 6. Fumarate treatment induces HO-1 in DCs and inhibits IL-12/IL-23p40 production by DCs in vivo.** (A–C) Mice were treated for 5 d with DMF in water or received DMF-free water (control). DCs were isolated, positively sorted, and stimulated with LPS for 18 h before analyzing HO-1 mRNA (A) or IL-12/IL-23p40 mRNA (B) expression by quantitative RT-PCR. RT-PCR data were normalized to β-actin levels, and expression in control mice was set as 1.0 (open bars). (C) DC isolated from DMF-treated or control mice were stimulated with LPS for 18 h, and IL-12p70 production was determined by ELISA. All data are shown as mean ± SEM and are representative for four independent experiments.

differentiation into either Th1 or Th17 cells. GATA3 remained at background levels (Fig. 7, A and B). In contrast, priming of CD4+ T cells with DMF-treated DCs induced GATA3 mRNA and protein expression, whereas T-bet or ROR-γt remained at background levels (Fig. 7, A and B). Modulation of GATA3, T-bet, or ROR-γt with fumarates strictly required DCs, as fumarates affected none of these transcription factors in highly purified CD4+ T cells stimulated with anti-CD3/anti-CD28 mAb in the absence of APCs (Figs. S3 and S4 A). DMF-treated DCs also primed CD4+ T cells to develop a classical Th2 cell phenotype that produced IL-4 instead of IFN-γ or IL-17 (Fig. 7, C and D) and showed no increase in Foxp3+ T cells, regardless of whether T cells were restimulated with APCs and peptide or with anti-CD3/anti-CD28 mAb (not depicted). In sharp contrast, when purified T cells were primed with anti-CD3/CD28 mAb, the addition of fumarates did not affect Th1, Th17, or Th2 cell differentiation (Figs. S3 and S4), confirming the strict requirement of APCs for the induction of Th2 cells with fumarates.

## Fumarate-induced type II DCs protect against EAE

Type II DCs impair the capacity of autoreactive T cells to induce organ-specific autoimmune disease (Menges et al., 2002; Schuler et al., 2003; Weber et al., 2007). As fumarate-induced type II DCs share all major features with classical type II DCs, fumarate-treated DCs should suppress Th1 and Th17 cell development in vivo, promote Th2 cell development, and abrogate the capacity of T cells to mediate organ-specific autoimmune diseases such as EAE (Racke et al., 1994; Chora et al., 2007). We started with the analysis of Vβ8.2 transgenic CD4+ T cells from B10.PL mice. Vβ8.2 transgenic CD4+ T cells that were stimulated with APCs and Ac1-11 peptide in the presence of MMF developed a Th2 phenotype and transferred only minimal disease. In contrast, Vβ8.2 transgenic CD4+ T cells differentiated in the absence of MMF transferred severe EAE (Fig. S5, A and B). We next analyzed in vitro the effects of DMF-induced type II DCs on the differentiation of in vivo primed CD4+ T cells. We isolated CD4+ T cells from SJL mice immunized with PLP139-151 peptide in CFA. When stimulated with peptide and DMSO-treated DCs, these PLP-specific CD4+ T cells developed a phenotype composed of Th1 and Th17 cells (Fig. S6, A and B) that transferred severe EAE (Fig. 7 E). Yet, when primed with DMF-induced type II DCs, the PLP-specific CD4+ T cells developed a Th2 phenotype (Fig. S6, A and B) that failed to adoptively transfer EAE (Fig. 7 E).

## Fumarates induce IL-12−IL-23− type II DCs in vivo

As DMF improves psoriasis (Altmeyer et al., 1994; Ghoreschi et al., 2003a) and MS (Kappos et al., 2008) in humans, we analyzed the effects of DMF therapy on APCs, T cell differentiation, and EAE in vivo. As predicted by the in vitro cell cultures, DMF treatment significantly diminished GSH in mice in vivo (Fig. S7 A). To determine the consequences of DMF treatment on the development of immune responses
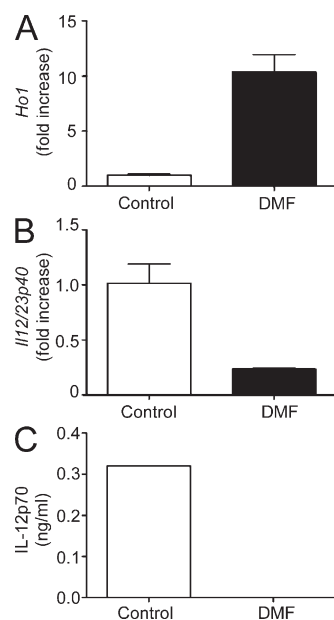
in vivo, we first immunized either DMF-treated or control SJL mice with PLP139-151 in CFA. On days 1–3, we quantified IL-12/IL-23p40, IL-12p35, or IL-23p19, T-bet, ROR-γt, or GATA3 mRNA (Fig. 8, A and B) and, on day 6, T cell differentiation in draining lymph nodes. Immunizing control mice with PLP139-151 in CFA induced mRNA expression of IL-12/IL-23p40, IL-12p35, and IL-23p19 (Fig. 8 A) and of T-bet and ROR-γt, whereas GATA3 remained low (Fig. 8 B). In sharp contrast, immunization of DMF-treated mice with PLP139-151 in CFA increased GATA3 mRNA ≥40-fold, whereas IL-12/IL-23p40, IL-12p35, IL-23p19, T-bet, or ROR-γt expression remained close to background (Fig. 8, A and B). Importantly, separate analysis of DCs and T cells isolated from DMF-treated nonimmunized mice had shown that DMF targeted the differentiation of DCs but not of T cells (Fig. 6 and not depicted). Intracellular cytokine staining and ELISPOT assays demonstrated that PLP139-151–specific CD4+ T cells from DMF-treated immunized mice were Th2 cells, whereas CD4+ T cells from immunized control mice showed a Th1 or Th17 phenotype (Fig. S7, B and C). These Th2 cells produced IL-4 but no IFN-γ, regardless of whether they were stimulated with PMA and ionomycin or with peptide and APCs. Controls had equivalent numbers of cytokine-producing PLP139-151–specific CD4+ T cells; yet, these CD4 T cells released IFN-γ but no IL-4 (Fig. S7, B and C). Consequently, DMF treatment induced functional type II DCs with relevant suppression of IL-12 and IL-23 in vivo (Fig. 8 A).

### In vivo induction of autoreactive Th2 cells by fumarate therapy protects against EAE

T cell priming during DMF therapy induced PLP-specific Th2 cells in vivo. To test whether this influenced the course of EAE, we compared the course of EAE in control mice and DMF-treated mice. Immunizing control mice with PLP139-151 in CFA resulted in severe, grade 4 EAE. In sharp contrast, DMF-treated mice were highly protected from EAE when immunized with PLP139-151 in CFA. Mice developed either no or only minimal signs of EAE (Fig. 8 C). Both, DMF and MMF treatment similarly protected SJL, B10.PL, and C57BL/6 mice from EAE whether we used active or passive immunization (not depicted).

To determine whether in vivo priming during fumarate treatment induced functional type II DCs that abolished the capacity of autoreactive T cells to cause EAE, we performed two different sets of experiments: we first asked whether DMF requires the induction of IL-4 to suppress EAE and then whether this suppression results from the IL-4–producing
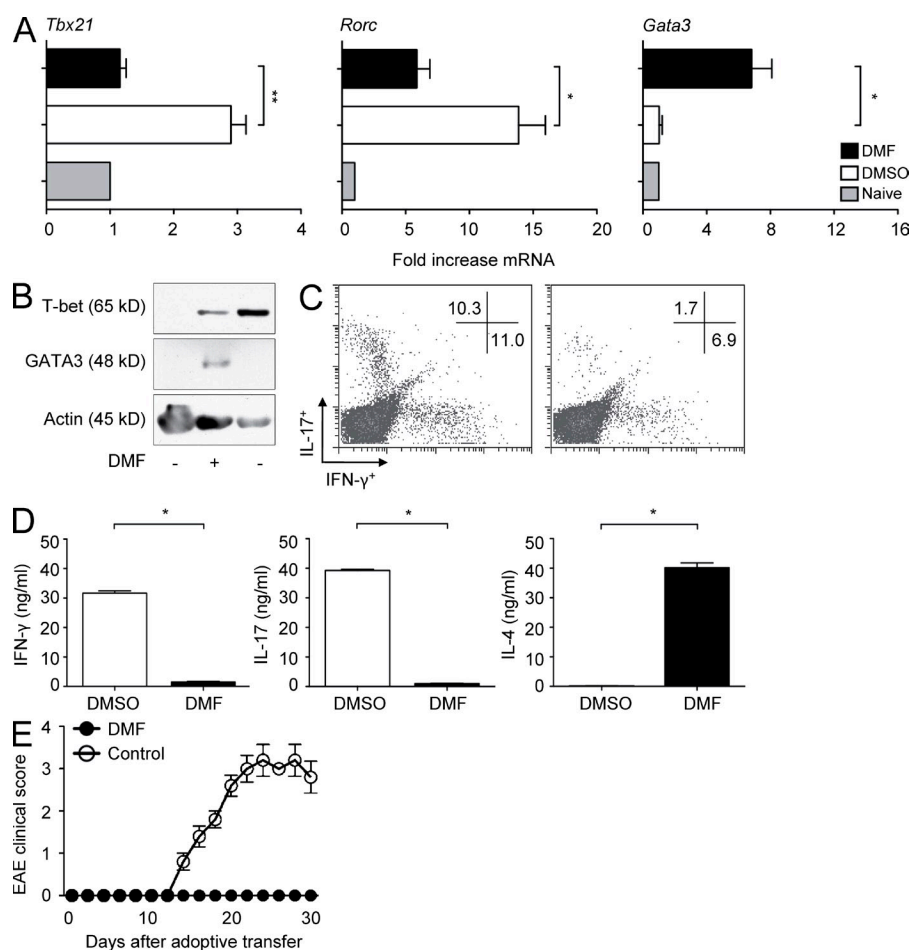


**Figure 7. Type II DCs resulting from fumarate treatment selectively induce Th2 cells in vitro.** (A) Naive OVA-specific CD4+ T cells were left unstimulated (gray bars) or were primed in vitro with OVA peptide and LPS-activated, DMSO-treated (open bars), or DMF-treated (black bars) DCs. Expression of the indicated transcription factors was assessed by RT-PCR, and the data were normalized to β-actin. Expression levels in unstimulated T cells were set at 1.0 (gray bars). Data are representative of three independent experiments (mean ± SEM; *, P < 0.05; **, P < 0.01). (B) DCs were treated and activated as in A and incubated alone (left lane) or with OVA-specific CD4+ T cells (middle and right lanes). T-bet or GATA3 protein expression in cell extracts was analyzed by Western blotting. (C and D) Naive OVA-specific CD4+ T cells were primed in vitro with OVA peptide and LPS-activated APCs in the presence or absence of DMF. Cells were expanded for 1 wk and then restimulated with OVA peptide and fresh APCs. Cytokines were determined by intracellular cytokine staining and flow cytometry (C) or by ELISA (D). Data from one representative experiment of three are shown (mean ± SEM; *, P < 0.001). (E) CD4+ T cells from immunized SJL mice were primed in vitro with PLP139-151 and APCs in the presence of DMF or DMSO (control) for 1 wk, restimulated, and expanded. 10^7 T cells were transferred into syngeneic WT mice (n = 5 per group), and EAE scores were determined. Data from one representative experiment of three are shown. Error bars represent SEM.

Th2 cells. We first induced EAE in either WT mice or IL-4–deficient (IL-4 KO) mice with MOG35-55 peptide and followed the course of disease in either control mice or DMF-treated mice. Without DMF treatment, both WT as well as IL-4 KO mice developed severe EAE (Fig. S8 A). Importantly, DMF treatment protected only WT mice from severe encephalomyelitis, whereas DMF treatment did not protect mice that were deficient in IL-4 (Fig. S8 B). This directly demonstrates that clinically effective DMF required the induction of IL-4–producing cells to protect against EAE.

To determine whether antigen-specific Th2 cells can mediate this protection, we primed TCR Vβ8.2 transgenic B10.PL mice with myelin basic protein (MBP) Ac1-11 peptide in CFA. Immunization of control mice resulted in severe EAE, and five out of eight animals died (Fig. 8 D).

Even in the presence of an expanded number of MBP-reactive CD4+ T cells, fumarate treatment improved EAE (P < 0.01 over 30 d), some mice even remained healthy (Fig. 8 D), and all survived. Subsequently, we isolated the transgenic

T cells from both groups of mice on day 42. CD4+ T cells from both groups of mice proliferated equally in response to peptide (not depicted), confirming that fumarate therapy induced fully functioning Th2 cells producing elevated levels of IL-4 and IL-10, rather than T reg cell or CD4+ T cell depletion (Fig. S7 D). We then transferred equal numbers of these in vivo primed T cells from both groups into naive recipients. The cells from diseased mice induced severe EAE (Fig. 8 E). In sharp contrast, CD4+ T cells from mice immunized during fumarate treatment developed a Th2 phenotype that failed to induce EAE in naive mice (grade ≤1; Fig. 8 E), directly showing that in vivo priming with the type II DCs abolished their capacity to cause EAE.

## DISCUSSION
As DMF is one of the first small molecules effective in the treatment of both MS and psoriasis, analyzing the mode of action of fumarates should unravel key mechanisms underlying both diseases. It further opens a platform to search for
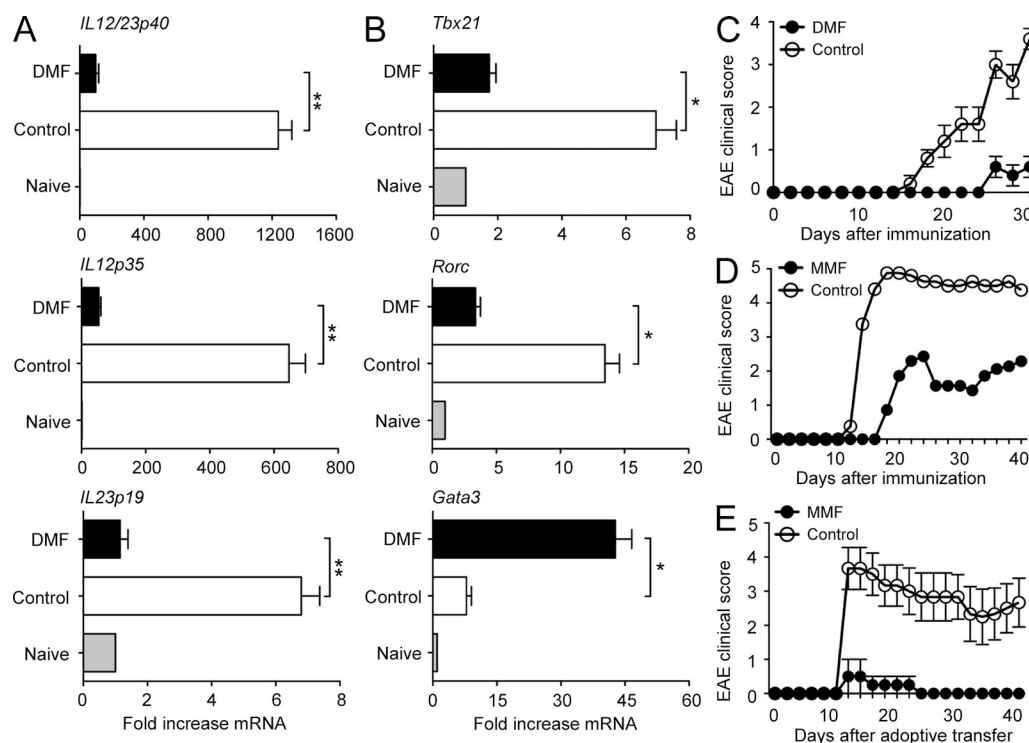


Figure 8. Fumarates induce type II APCs and Th2 cells in vivo and abolish the capacity of autoreactive CD4+ T cells to induce EAE. (A and B) SJL mice received DMF or DMF-free (control) water and were immunized with PLP139-151 peptide in CFA. On days 1–3, draining lymph nodes were isolated, RNA was extracted, and IL-12/IL-23p40, IL-12p35, or IL-23p19 expression (A) or Tbx21, Rorc, or Gata3 expression (B) was analyzed by RT-PCR (mean ± SEM; **, P < 0.001). Data were normalized to β-actin levels, and expression in naive mice was set as 1.0 (gray bars). Data from one representative experiment of three are shown (*, P < 0.01). (C) SJL mice were fed with DMF-containing or -free (control) water and immunized with PLP139-151 peptide in CFA and pertussis toxin (n = 5 per group). Clinical EAE scores were determined at the indicated times after immunization. Data are from one representative experiment of four. (D) TCR Vβ8.2 transgenic B10.PL mice were fed with 5 mg MMF or MMF-free (control) water (n = 8 per group). Mice were then immunized with MBP Ac1-11 peptide in CFA, and clinical scores were assessed at the indicated times after immunization. EAE incidence was 8/8 for control mice and 6/8 in the MMF group. (E) CD4+ T cells were isolated from spleens of MMF-treated or control donors from D on day 42, and equal numbers of cells (10^7) were adoptively transferred into naive mice. EAE scores were assessed at the indicated times after adoptive transfer (MMF group, n = 4; control group, n = 6). Experiments with MMF were performed four times in B10.PL or SJL mice, and data shown are from one representative experiment. (C and E) Error bars represent SEM.

novel therapeutic strategies. Four major conclusions result from our data. (1) Intracellular concentrations of GSH, the main intracellular ROS scavenger, determine whether immune responses differentiate into either a Th1/Th17 or a Th2 phenotype. (2) In vitro and direct ex vivo analysis of DCs and T cells demonstrate that the inhibition of Th1/Th17 cells and the induction of Th2 cells result from the induction of type II DCs and not from direct modulation of T cell differentiation. (3) GSH depletion induces type II DCs by affecting two distinct signaling cascades: induction of HO-1 impairs production of IL-23, whereas silencing of STAT1 phosphorylation impairs IL-12 production. (4) Immune deviation, based on the active induction of autoreactive Th2 cells, is a valid approach for the treatment of inflammatory autoimmune diseases mediated by autoreactive Th1 and Th17 cells.

Based on the observation that different GST genotypes are closely associated with distinct serum IgE levels and the risk of ROS-triggered type I allergy on the one hand (Gilliland et al., 2004) and the observation that ROS stress impairs IL-12 production (Peterson et al., 1998) on the other, we hypothesized that DMF might exert the antiinflammatory effects by inducing type II DCs through GSH depletion. Depending on the experimental conditions, DMF was reported to either decrease or increase GSH levels (Mrowietz and Asadullah, 2005). To determine the significance of DMF-induced GSH depletion and the resulting ROS stress for induction of type II DCs, we first compared DMF and MMF with $H_2O_2$ and restored GSH with GSH-OEt or NAC. DMF, MMF, or $H_2O_2$ had identical effects on the cytokine production by DCs (unpublished data), and the effects were fully reversed by GSH-OEt or NAC. Thus, GSH depletion by DMF generated type II DCs that produced IL-10 instead of IL-12 or IL-23 and that induced Th2 instead of Th1 and Th17 cells. Similar to DMF, another drug used for the treatment of MS, glatiramer acetate, can deviate Th1 into Th2 responses in mice and in humans. Like DMF, glatiramer acetate induces immune deviation by inducing type II APCs that subsequently favor T cell differentiation toward a Th2 phenotype and ameliorate EAE (Weber et al., 2007). Although induction of type II APCs appears to be a viable mechanism for ameliorating autoimmune disease (Racke et al., 1994; Schuler et al., 2003; Chora et al., 2007; Weber et al., 2007), the underlying molecular mechanisms that result in type II APCs remain unclear (Kapsenberg, 2003). As various modes of ROS stress, including CO exposure, suppress Th1 development without inducing T reg cells (Hegazi et al., 2005; Nakahira et al., 2006; Chora et al., 2007), we analyzed the effects of ROS on the signaling pathways that are involved in the differentiation of Th1, Th17, and Th2 responses. Importantly, DMF affected T-bet, ROR-γt, and GATA3 only in CD4$^+$ T cells stimulated by antigen and APCs. DMF had no effect on CD4$^+$ T cells stimulated with anti-CD3/CD28 mAb in the absence of APCs. These experimental conditions revealed that DMF affected T cells only indirectly. This was confirmed by in vivo data. Freshly isolated CD4$^+$ T cells

from unprimed but either DMF-treated or control mice had equivalent numbers of IFN-γ–, IL-17–, or IL-4–producing CD4$^+$ T cells after polyclonal stimulation (unpublished data). In sharp contrast, freshly isolated DCs from DMF-treated mice differed from DCs of control mice. DCs from DMF-treated mice had increased HO-1 mRNA expression and significantly reduced IL-12 and IL-23 mRNA expression and cytokine production when stimulated with LPS. Thus, DMF caused immune deviation in vitro and in vivo by inducing type II DCs. The powerful DMF-mediated suppression of STAT1 phosphorylation in DCs provided an important link. This significance was supported by the suppression of ICSBP/IRF-8, an IL-12–regulating transcription factor directly downstream of IFNs and STAT1. Moreover, DCs from STAT1$^{-/-}$ mice failed to produce substantial amounts of IL-12. As GSH–depleting small molecules as well as glatiramer acetate have previously been connected with STAT1 signaling (Weber et al., 2007; Kim et al., 2008), one mode of inducing type II DCs with DMF may be the ROS-mediated prevention of STAT1 phosphorylation in APCs. However, STAT1$^{-/-}$ and IL-12p35$^{-/-}$ mice develop more severe EAE than WT mice (Becher et al., 2002; Bettelli et al., 2004).

As IL-23p19$^{-/-}$ mice are resistant to EAE, prevention of STAT1 phosphorylation may suppress IL-12 production, without interfering with IL-23. Indeed, DCs from STAT1$^{-/-}$ mice produced normal amounts of IL-23, a finding which may explain the increased disease severity of EAE in STAT1$^{-/-}$ mice. It further shows that DMF-mediated oxidative stress impairs IL-23 production and EAE through pathways different from impaired STAT1 signaling alone.

In line with others, we found no major response of Nrf2 mRNA to ROS (Durchdewald et al., 2007). As HO-1 is a classical ROS-sensitive heat shock protein (Keyse and Tyrrell, 1989), we speculated that ROS stress should enhance TLR-mediated induction of HO-1, a molecule associated with inhibition of EAE (Chora et al., 2007) and of experimental IBD (Hegazi et al., 2005). Indeed, DMF treatment of human PBMCs promotes HO-1 mRNA and protein production in response to TLR stimuli, and HO-1 siRNA partially restores IL-12/IL-23p40 expression in DMF-treated PBMCs (Lehmann et al., 2007). In addition, HO-1$^{-/-}$ mice share with STAT1$^{-/-}$ or IL-12p35$^{-/-}$ mice an exacerbated course of EAE (Chora et al., 2007; Tzima et al., 2009). We therefore hypothesized that HO-1 might negatively regulate IL-23p19. Indeed, HO-1 siRNA was able to restore IL-23p19 mRNA production and, partially, IL-12/IL-23p40, while leaving IL-12p35 unaffected. In line with others (Lin et al., 2007), we also found that in DCs, conditions that induce HO-1 result in translocation of a truncated, N-terminal part of HO-1 into the nucleus. Interestingly, in DCs treated with DMF, nuclear HO-1 physically associates with AP-1– and NF-κB–binding sites of the promoter region of IL-23p19. This is of biological significance, as nuclear HO-1 interferes with the transcriptional activity of AP-1 and NF-κB (Lin et al., 2007). In line with these studies, we found that HO-1 interacts with NF-κB–binding sites of the IL-23p19 promoter, thereby

directly suppressing the promoter activity of IL-23p19. In contrast, HO-1 does apparently not affect the binding of STAT1 (Chora et al., 2007; Lin et al., 2007) or of IL-12p35 expression. Nonetheless, we and others (Chora et al., 2007) found that ROS stress simultaneously activates HO-1 and impairs STAT1 phosphorylation. This strongly suggests that DMF or other ROS-inducing molecules generate type II DCs through GSH depletion that subsequently impairs the production of both IL-12 and IL-23 by interfering with two independent signaling pathways. Such type II DCs promote Th2 cells while impairing both Th1 and Th17 development. This may also explain why various molecules like glatiramer acetate (Weber et al., 2007), CO, or CoPPIX (Hegazi et al., 2005; Nakahira et al., 2006), which improve the Th1 and Th17 cell–driven autoimmune diseases EAE or IBD in mice, simultaneously suppress IL-12, IFN-γ, STAT1 phosphorylation, and IL-23. The profound effect on these two signaling pathways may explain the efficacy of DMF in treating EAE, as shown here and in a related study (Schilling et al., 2006), and in treating different human diseases such as MS (Kappos et al., 2008) and psoriasis (Altmeyer et al., 1994). In addition to their effects on oxidative stress–related pathways in DCs, fumarates may influence related metabolic or signaling pathways in other cell types such as monocytes, neurons, or endothelia (Ghashghaeinia et al., 2010; Arbiser, 2011; Linker et al., 2011).

If targeting of the IL-12/IL-23 pathways by small GSH-regulating molecules is effective in the treatment of different autoimmune diseases in mice and even in humans, one may ask why mAb against IL-12/IL-23p40 led to disappointing results in patients with MS (Segal et al., 2008). No studies have been performed to evaluate IL-12p35, IL-23p19, and IL-10 production by APCs in anti–IL-12/IL-23p40–treated humans and mice. Additionally, early intervention may be important when treating MS with anti–IL-12/IL-23p40 antibodies. In sharp contrast, GSH depletion with the small molecule DMF directly inhibited IL-12p35 and IL-23p19 and generated classical type II DCs that, like glatiramer acetate, induced autoreactive Th2 cells. This is in line with the effects of recombinant IL-4 in attenuating delayed type hypersensitivity reactions in mice, such as EAE (Racke et al., 1994), contact hypersensitivity (Biedermann et al., 2001a), or control of parasite infection (Biedermann et al., 2001b), or on psoriasis in humans (Ghoreschi et al., 2003b), where continuous supply of IL-4 significantly improved Th1/Th17 diseases in a dose-dependent fashion. This suggests that successful treatment of autoimmune diseases such as MS and psoriasis requires not only neutralization of IL-12 and IL-23 by mAb but also the alteration of the pathogenic T cells via DCs. The data fit best with a model in which treatment of MS requires, in addition to the inhibition of IL-12 and IL-23, immune deviation and the active induction of protective Th2 cells either by IL-4 (Racke et al., 1994) or by type II DCs. This is supported by the unique efficacy of IL-4 in the treatment of various inflammatory model diseases in mice (Racke et al., 1994; Biedermann et al., 2001a,b), the treatment

of psoriasis in humans (Ghoreschi et al., 2003b), and the unique efficacy of DMF and glatiramer acetate, two small molecules which are both effective in MS (Weber et al., 2007; Kappos et al., 2008), to impair IL-12 and IL-23 and, in addition, deviate Th cell responses toward a Th2 phenotype.

## MATERIALS AND METHODS

**Psoriasis therapy with fumarates.** PBMCs were isolated from 19 patients studied who received DMF (720 mg/day) or placebo during a controlled, randomized double-blind trial (FAG-201; Fumapharm/Biogen Idec) for severe psoriasis (psoriasis area and severity index ≥ 12 at baseline). Intracellular cytokine staining and flow cytometry were performed from accessible patient samples at the indicated time points. CD14+ monocytes from healthy donors were isolated by MACS separation (Miltenyi) and differentiated into DCs with 1,000 U/ml GM-CSF and 500 U/ml IL-4 for 7 d before activation with 1 mg/ml LPS. The study protocol, patient documentation, and blood analysis were approved by the ethics committees of the Eberhard Karls University Tübingen and the Ludwig-Maximilians University Munich.

**Mice.** Female BALB/c, C57BL/6, C57BL/6-$Il4^{-/-}$, B10.PL, SJL/J, STAT1$^{-/-}$ Sv129SvEv, TCR Vβ8.2 B10.PL, and DO11.10 TCR transgenic mice were purchased (The Jackson Laboratory, Charles River, and Harlan-Winkelmann) and maintained in the animal facilities of the University of Texas Southwestern Medical Center, the Ohio State University Medical Center, or the Eberhard Karls University Tübingen under specific pathogen-free conditions. Animal experiments were approved by the Institutional Animal Care and Use Committee of the University of Texas Southwestern, the Ohio State University, or Regierungspräsidium Tübingen.

**GSH determination.** Cellular GSH and GSH disulfide were determined in microtiter plate assays using a colorimetric method (Dringen and Hamprecht, 1996). GSH disulfide was repeatedly not increased in the cells exposed to fumarates.

**Quantifying ROS.** BMDCs were treated with vehicle (DMSO) alone or with 70 µM DMF or in combination with 1 mM GSH-OEt or with 1 mM NAC. After incubation for 2–4 h at 37°C, DCs were stained with 1 mM 2',7'dichlorofluorescein (H$_2$DCFDA; Invitrogen) for 30 min, washed with PBS, and analyzed by flow cytometry (FACSCalibur; BD), using CellQuest (BD) and FCS Express software (De Novo Software).

**Cytokine assays.** ELISA sets or single components were used for quantification of IL-4, IL-10, IL-12, and IFN-γ (BD), IL-23 (eBioscience), and IL-17 (R&D Systems). Intracellular cytokine staining was performed as described previously (Ghoreschi et al., 2003b). Cells were stimulated with PMA/ionomycin or APCs/peptide. Data are presented as one representative of three independent experiments with similar results.

**ELISPOT.** CD4+ T cells from draining lymph nodes were stimulated for 48 h with APCs and 10 µg/ml peptide in HA plates (Millipore) coated with 10 µg/ml anti–IFN-γ or anti–IL-4 mAb (BD). Bound cytokines were visualized by incubation with biotinylated anti–IFN-γ or anti–IL-4 mAb (BD), followed by the addition of streptavidin-AP conjugate (Boehringer Ingelheim) in PBS/Tween and premixed alkaline phosphatase substrate (SigmaFast; Sigma-Aldrich) as described previously (Ghoreschi et al., 2003b). Spots were counted using a bioreader system (BIOSYS) and expressed as mean number of spots ± SEM of triplicate determinations. Spots were calculated as the difference between T cells cultured with peptide and T cells cultured with APCs only. Experiments were performed three times.

**APCs and peptides.** T cell–depleted spleen cells (APCs) or day 7 BMDCs were prepared as described previously (Lutz et al., 1999) and cultured either in medium alone with DMSO (C$_2$H$_6$OS), 70 µM DMF (C$_6$H$_8$O$_4$; dissolved in DMSO), and 1 mM GSH-OEt (C$_{12}$H$_{21}$N$_3$O$_6$S; all from Sigma-Aldrich)

or 50 µM MMF ($CaC_{10}H_{10}O_8$; Fumapharm). At the indicated time, cells were either directly analyzed for intracellular GSH content and protein quantification or used for cytokine analysis or for T cell stimulation. For stimulation through TLR4, we incubated cells with 1 µg/ml of *Escherichia coli* LPSs 055:B5 (Sigma-Aldrich). OVA323–339 peptide (ISQAVHAA-HAEINEAGR), PLP139-151 peptide (HCLGKWLGHPDKF) and MOG35-55 peptide (MEVGWYRSPFSRVVHLYRNGK) were purchased from EMC Microcollections, and MBP Ac1-11 peptide (ASQKRPSQRSK) was purchased from CS Bio Company.

**T cell cultures.** $CD4^+$ T cells were primed for 2 d with peptide and BMDCs or APCs, expanded for 7–8 d with 50 U/ml IL-2 (Chiron Therapeutics), and restimulated with either peptide and APCs for cytokine release into supernatants or with PMA/ionomycin for intracellular cytokine staining. Alternatively, purified $CD4^+$ T cells were stimulated with plate-bound anti-CD3 mAb and 2 µg/ml soluble anti-CD28 mAb (BD) and expanded for 7–8 d with IL-2.

**Myelin antigen–specific T cells and EAE induction.** $CD4^+$ T cells from spleen and lymph nodes of immunized SJL mice were stimulated with 10 µg/ml PLP139-151 and irradiated syngeneic APCs or DCs in the presence of DMSO or of 35–70 µM DMF in DMSO for 2–3 d, expanded for 1 wk with IL-2, and then restimulated for cytokine production. For adoptive transfer, we injected $10^7$ T cells, primed with either DMSO- or DMF-treated APCs, intraperitoneally into syngeneic naive mice and monitored EAE score (Racke et al., 1994). Active EAE was induced by immunization of either TCR transgenic B10.PL mice with 400 µg MBP Ac1-11 peptide in CFA, by subcutaneous injection of SJL mice with 75 µg PLP139-151 in CFA, or by subcutaneous injection of C57BL/6 or C57BL/6-$Il4^{-/-}$ mice with 75 µg MOG35-55 in CFA. Mice received 200 ng pertussis toxin on days 0 and 2, and SJL mice received pertussis toxin on day 0 only. GSH depletion was induced by feeding mice either 5 mg MMF or 1.5 mg DMF in saline-containing water daily for 10–14 d as described previously (Ghashghaeinia et al., 2010). Control mice were fed with fumarate-free saline-containing water. Clinical assessment of EAE was performed using the following scale: 0, no disease; 1, limp tail; 2, hind limb weakness or partial paralysis; 3, complete hind limb paralysis; 4, forelimb and hind limb paralysis; 5, moribund state.

**Gene expression analysis.** Ex vivo cytokine mRNA was determined without restimulation. Total RNA from indicated tissue or cells was isolated by standard methods and reverse transcribed. Quantitative RT-PCR was performed using the LightCycler 480 and SYBR green (Roche) or TaqMan probes (TIB MOLBIOL). β-Actin levels were measured in the same PCR reaction. Individual RT-PCR reactions were performed in 10-µl volumes in a 96-well plate. The relative gene expression of *Il12p35*, *Il12/Il23p40*, *Il23p19*, *Rorc*, *Gata3*, *Tbx21*, and *Ho1* was calculated against the expression of β-actin. Only samples with appropriate dissociation curves were considered for analysis.

**Western blot analysis.** BMDCs or the indicated cell combinations were incubated as given in the figure legends. Cells were washed with ice-cold PBS before lysates were separated by SDS-PAGE and blotted onto polyvinylidenefluoride membranes. STAT1, phospho-STAT1 (Tyr701), p44/42 MAPK, and phospho-p38 MAPK (Thr180/Tyr182) were detected with rabbit pAbs (dilution 1:1,000; Cell Signaling Technology) and T-bet or GATA3 with antibodies from Santa Cruz Biotechnology, Inc. Immunoblots were visualized by incubation with horseradish peroxidase–conjugated goat anti–rabbit IgG (dilution 1:2,000; Cell Signaling Technology) followed by enhanced chemiluminescence (GE Healthcare). For analysis of HO-1 expression, cell extracts were separated into nuclear or cytoplasmic fractions, and blots were incubated with antibodies directed against C-terminal HO-1 (M-19; Santa Cruz Biotechnology, Inc.) or N-terminal HO-1 protein (SPA-896; Enzo Life Sciences).

**Transfection with siRNA.** siRNA transfection was performed in Opti-MEM serum-free medium (Invitrogen). To form complexes, the cationic lipid and siRNA (HO-1 or control; Thermo Fisher Scientific) were each diluted in Opti-MEM incubated at room temperature and then added to the cells as suggested by the manufacturer. After 24 h, medium was removed, and mRNA or protein analysis was performed 24–72 h after transfection.

**Overexpression of HO-1.** E1- and E3-deleted adenoviral vectors expressing EGFP or mouse HO-1–EGFP were a gift from T. Tüting (University of Bonn, Bonn, Germany) and J.W. Kupiec-Weglinski (University of California, Los Angeles, Los Angeles, CA). All recombinant adenoviruses were based on Ad5 and contained the transgene under the control of the CMV immediate–early promoter. Viruses were propagated in 293 cells, purified by cesium chloride density gradient centrifugation and subsequent dialysis according to standard protocols, and stored at 70°C. Adenoviruses were added to DC cultures on day 8 at a multiplicity of infection of 300. Cells were incubated for 2 h at 37°C and 7.5% $CO_2$ before stimulation with LPS for 1 h. Infection efficiency was confirmed by flow cytometry and Western blot analysis of HO-1.

**ChIP and RT-PCR.** ChIP was performed as described previously (Rothfuss et al., 2009). In brief, DMF-treated or control DCs were activated with LPS, cross-linked, harvested, and lysed by sonication. Cell lysates were immunoprecipitated with anti–HO-1 (Cell Signaling Technology) or anti–acetyl H3 (Millipore) antibodies. The eluted DNA was purified, and samples were analyzed by quantitative PCR. Primers were designed to amplify 150–250-bp fragments from selected genomic regions. RT-PCR was performed in duplicate on each sample and input DNA using LightCycler 480 SYBR Green I Master mix (Roche) according to manufacturer's instructions in a LightCycler 480 system (Roche). The product specificity was monitored by melting curve analysis, and product size was visualized on agarose gel by electrophoresis. Equal quantities of sample and input DNA were used for each real-time amplification. To account for the differences in DNA quantity, for every genomic sequence studied, a ΔCt value was calculated for each sample by subtracting the Ct value of the chromatin immunoprecipitated sample from the Ct value obtained for the input and no antibody ChIP, respectively. Calculating $2^{ΔΔCt}$ yielded the relative amount of PCR product (relative enrichment). Binding sites for AP-1 and NF-κB within the IL-23p19 promoter region were identified with Gene2Promoter (Genomatix). Primers were designed with Primer3 or used as published previously (Mise-Omata et al., 2007; Liu et al., 2009): AP-1 site (P1) forward, 5′-CCAA-AGAGGGAGATGATGTAGGG-3′; and reverse, 5′-AATCCAGCATC-TTGTTCCCTG-3′; NF-κB (c-Rel) site (P2) forward, 5′-GGCTCTCCA-AAGAGGGAGAT-3′; and reverse, 5′-AAGCGGCTTCCTGATTTCTT-3′; NF-κB (RelA/c-Rel) site (P3) forward, 5′-GGCTCTCCAAAGAGG-GAGAT-3′; and reverse, 5′-CCACCTCCTTTGGTTCTGAG-3′; and control forward, 5′-TTGCAGAAGATGTGGGTTCA-3′; and reverse, 5′-CCACTTGGAAACATGCAGTC-3′.

**Luciferase reporter gene assays.** The p19 luciferase construct was a gift from Y. Chen (University of Pennsylvania, Philadelphia, PA; Carmody et al., 2007). RAW246.7 cells were transfected with a pGL3-*Il23p19* reporter plasmid (bp −1180/+110 promoter fragment). After transfection with Lipofectamine reagent, cells were treated with the indicated concentrations of DMF and activated with 100 ng/ml LPS. The cells were harvested with reporter lysis buffer (Promega) and assayed for luciferase activity. NIH 3T3 cells were transfected with a pGL3-IL23p19 reporter plasmid (bp −560/+104; Kortylewski et al., 2009) together with the expression vectors for mouse p65/RelA (plasmid 20012; Addgene) and the indicated amounts of mouse HO-1 and pRSV-βGal. Plasmid concentrations were adjusted with empty expression vector to achieve equal amounts of total DNA. Transfection was performed using jetPEI (Peqlab) according to the manufacturer's protocol, and 48 h after transfection, cells were harvested and luciferase assays were performed as described previously (Graupner et al., 2011). Activity of cotransfected β-galactosidase was used to normalize reporter gene induction.

**Statistical analysis.** We examined significance between groups using the two-tailed Student's *t* test for paired or unpaired samples.

**Online supplemental material.** Fig. S1 shows suppression of IL-23p19 through HO-1 overexpression. Fig. S2 shows the fumarate-induced type II phenotype in DCs from various mouse strains. Fig. S3 shows fumarate-induced GATA3 and suppressed T-bet expression in T cells and the importance of the presence of APCs. Fig. S4 shows fumarate-mediated induction of Th2 cells by type II DCs. Fig. S5 shows that fumarate-induced Th2 cells in vitro are not pathogenic after transfer in vivo. Fig. S6 shows that fumarates induce a Th2 phenotype in PLP-specific T cells. Fig. S7 shows that fumarates deplete GSH and induce type II DCs and Th2 responses in vivo. Fig. S8 shows that fumarates protect from severe encephalomyelitis in WT mice but not in IL-4–deficient mice. Online supplemental material is available at http://www.jem.org/cgi/content/full/jem.20100977/DC1.

## REFERENCES

Altmeyer, P.J., U. Matthes, F. Pawlak, K. Hoffmann, P.J. Frosch, P. Ruppert, S.W. Wassilew, T. Horn, H.W. Kreysel, G. Lutz, et al. 1994. Antipsoriatic effect of fumaric acid derivatives. Results of a multicenter double-blind study in 100 patients. *J. Am. Acad. Dermatol.* 30:977–981. http://dx.doi.org/10.1016/S0190-9622(94)70121-0

Arbiser, J.L. 2011. Fumarate esters as angiogenesis inhibitors: key to action in psoriasis? *J. Invest. Dermatol.* 131:1189–1191. http://dx.doi.org/10.1038/jid.2011.45

Axtell, R.C., B.A. de Jong, K. Boniface, L.F. van der Voort, R. Bhat, P. De Sarno, R. Naves, M. Han, F. Zhong, J.G. Castellanos, et al. 2010. T helper type 1 and 17 cells determine efficacy of interferon-beta in multiple sclerosis and experimental encephalomyelitis. *Nat. Med.* 16:406–412. http://dx.doi.org/10.1038/nm.2110

Becher, B., B.G. Durell, and R.J. Noelle. 2002. Experimental autoimmune encephalitis and inflammation in the absence of interleukin-12. *J. Clin. Invest.* 110:493–497.

Bettelli, E., B. Sullivan, S.J. Szabo, R.A. Sobel, L.H. Glimcher, and V.K. Kuchroo. 2004. Loss of T-bet, but not STAT1, prevents the development of experimental autoimmune encephalomyelitis. *J. Exp. Med.* 200:79–87. http://dx.doi.org/10.1084/jem.20031819

Biedermann, T., R. Mailhammer, A. Mai, C. Sander, A. Ogilvie, F. Brombacher, K. Maier, A.D. Levine, and M. Röcken. 2001a. Reversal of established delayed type hypersensitivity reactions following therapy with IL-4 or antigen-specific Th2 cells. *Eur. J. Immunol.* 31:1582–1591. http://dx.doi.org/10.1002/1521-4141(200105)31:5<1582::AID-IMMU1582>3.0.CO;2-M

Biedermann, T., S. Zimmermann, H. Himmelrich, A. Gumy, O. Egeter, A.K. Sakrauski, I. Seegmüller, H. Voigt, P. Launois, A.D. Levine, et al. 2001b. IL-4 instructs TH1 responses and resistance to *Leishmania major* in susceptible BALB/c mice. *Nat. Immunol.* 2:1054–1060. http://dx.doi.org/10.1038/ni725

Burton, P.R., D.G. Clayton, L.R. Cardon, N. Craddock, P. Deloukas, A. Duncanson, D.P. Kwiatkowski, M.I. McCarthy, W.H. Ouwehand, N.J. Samani, et al. 2007. Association scan of 14,500 nonsynonymous SNPs in four diseases identifies autoimmunity variants. *Nat. Genet.* 39:1329–1337. http://dx.doi.org/10.1038/ng.2007.17

Carmody, R.J., Q. Ruan, H.-C. Liou, and Y.H. Chen. 2007. Essential roles of c-Rel in TLR-induced *IL-23 p19* gene expression in dendritic cells. *J. Immunol.* 178:186–191.

Chora, A.A., P. Fontoura, A. Cunha, T.F. Pais, S. Cardoso, P.P. Ho, L.Y. Lee, R.A. Sobel, L. Steinman, and M.P. Soares. 2007. Heme oxygenase-1 and carbon monoxide suppress autoimmune neuroinflammation. *J. Clin. Invest.* 117:438–447. http://dx.doi.org/10.1172/JCI28844

de Jong, R., A.C. Bezemer, T.P. Zomerdijk, T. van de Pouw-Kraan, T.H. Ottenhoff, and P.H. Nibbering. 1996. Selective stimulation of T helper 2 cytokine responses by the anti-psoriasis agent monomethylfumarate. *Eur. J. Immunol.* 26:2067–2074. http://dx.doi.org/10.1002/eji.1830260916

Dringen, R., and B. Hamprecht. 1996. Glutathione content as an indicator for the presence of metabolic pathways of amino acids in astroglial cultures. *J. Neurochem.* 67:1375–1382. http://dx.doi.org/10.1046/j.1471-4159.1996.67041375.x

Dudziak, D., A.O. Kamphorst, G.F. Heidkamp, V.R. Buchholz, C. Trumpfheller, S. Yamazaki, C. Cheong, K. Liu, H.W. Lee, C.G. Park, et al. 2007. Differential antigen processing by dendritic cell subsets in vivo. *Science.* 315:107–111. http://dx.doi.org/10.1126/science.1136080

Durchdewald, M., T.A. Beyer, D.A. Johnson, J.A. Johnson, S. Werner, and U. auf dem Keller. 2007. Electrophilic chemicals but not UV irradiation or reactive oxygen species activate Nrf2 in keratinocytes in vitro and in vivo. *J. Invest. Dermatol.* 127:646–653. http://dx.doi.org/10.1038/sj.jid.5700585

Frohman, E.M., M.K. Racke, and C.S. Raine. 2006. Multiple sclerosis—the plaque and its pathogenesis. *N. Engl. J. Med.* 354:942–955. http://dx.doi.org/10.1056/NEJMra052130

Gautier, G., M. Humbert, F. Deauvieau, M. Scuiller, J. Hiscott, E.E. Bates, G. Trinchieri, C. Caux, and P. Garrone. 2005. A type I interferon autocrine–paracrine loop is involved in Toll-like receptor-induced interleukin-12p70 secretion by dendritic cells. *J. Exp. Med.* 201:1435–1446. http://dx.doi.org/10.1084/jem.20041964

Ghashghaeinia, M., D. Bobbala, T. Wieder, S. Koka, J. Brück, B. Fehrenbacher, M. Röcken, M. Schaller, F. Lang, and K. Ghoreschi. 2010. Targeting glutathione by dimethylfumarate protects against experimental malaria by enhancing erythrocyte cell membrane scrambling. *Am. J. Physiol. Cell Physiol.* 299:C791–C804. http://dx.doi.org/10.1152/ajpcell.00014.2010

Ghoreschi, K., U. Mrowietz, and M. Röcken. 2003a. A molecule solves psoriasis? Systemic therapies for psoriasis inducing interleukin 4 and Th2 responses. *J. Mol. Med.* 81:471–480. http://dx.doi.org/10.1007/s00109-003-0460-9

Ghoreschi, K., P. Thomas, S. Breit, M. Dugas, R. Mailhammer, W. van Eden, R. van der Zee, T. Biedermann, J. Prinz, M. Mack, et al. 2003b. Interleukin-4 therapy of psoriasis induces Th2 responses and improves human autoimmune disease. *Nat. Med.* 9:40–46. http://dx.doi.org/10.1038/nm804

Gilliland, F.D., Y.F. Li, A. Saxon, and D. Diaz-Sanchez. 2004. Effect of glutathione-S-transferase M1 and P1 genotypes on xenobiotic enhancement of allergic responses: randomised, placebo-controlled crossover study. *Lancet.* 363:119–125. http://dx.doi.org/10.1016/S0140-6736(03)15262-2

Graupner, V., E. Alexander, T. Overkamp, O. Rothfuss, V. De Laurenzi, B.F. Gillissen, P.T. Daniel, K. Schulze-Osthoff, and F. Essmann. 2011. Differential regulation of the proapoptotic multidomain protein Bak by p53 and p73 at the promoter level. *Cell Death Differ.* 18:1130–1139. http://dx.doi.org/10.1038/cdd.2010.179

Hegazi, R.A., K.N. Rao, A. Mayle, A.R. Sepulveda, L.E. Otterbein, and S.E. Plevy. 2005. Carbon monoxide ameliorates chronic murine colitis through a heme oxygenase 1–dependent pathway. *J. Exp. Med.* 202:1703–1713. http://dx.doi.org/10.1084/jem.20051047

Jeannin, P., Y. Delneste, S. Lecoanet-Henchoz, J.F. Gauchat, P. Life, D. Holmes, and J.Y. Bonnefoy. 1995. Thiols decrease human interleukin (IL) 4 production and IL-4–induced immunoglobulin synthesis. *J. Exp. Med.* 182:1785–1792. http://dx.doi.org/10.1084/jem.182.6.1785

Kappos, L., R. Gold, D.H. Miller, D.G. Macmanus, E. Havrdova, V. Limmroth, C.H. Polman, K. Schmierer, T.A. Yousry, M. Yang, et al. 2008. Efficacy and safety of oral fumarate in patients with relapsing-remitting multiple sclerosis: a multicentre, randomised, double-blind, placebo-controlled phase IIb study. *Lancet.* 372:1463–1472. http://dx.doi.org/10.1016/S0140-6736(08)61619-0

Fumarates induce protective type II DCs | Ghoreschi et al.

Kapsenberg, M.L. 2003. Dendritic-cell control of pathogen-driven T-cell polarization. *Nat. Rev. Immunol.* 3:984–993. http://dx.doi.org/10.1038/nri1246

Keyse, S.M., and R.M. Tyrrell. 1989. Heme oxygenase is the major 32-kDa stress protein induced in human skin fibroblasts by UVA radiation, hydrogen peroxide, and sodium arsenite. *Proc. Natl. Acad. Sci. USA.* 86:99–103. http://dx.doi.org/10.1073/pnas.86.1.99

Kim, H.S., I.H. Cho, J.E. Kim, Y.J. Shin, J.H. Jeon, Y. Kim, Y.M. Yang, K.H. Lee, J.W. Lee, W.J. Lee, et al. 2008. Ethyl pyruvate has an anti-inflammatory effect by inhibiting ROS-dependent STAT signaling in activated microglia. *Free Radic. Biol. Med.* 45:950–963. http://dx.doi.org/10.1016/j.freeradbiomed.2008.06.009

Kneilling, M., R. Mailhammer, L. Hültner, T. Schönberger, K. Fuchs, M. Schaller, D. Bukala, S. Massberg, C.A. Sander, H. Braumüller, et al. 2009. Direct crosstalk between mast cell-TNF and TNFR1-expressing endothelia mediates local tissue inflammation. *Blood.* 114:1696–1706. http://dx.doi.org/10.1182/blood-2008-11-187682

Kortylewski, M., H. Xin, M. Kujawski, H. Lee, Y. Liu, T. Harris, C. Drake, D. Pardoll, and H. Yu. 2009. Regulation of the IL-23 and IL-12 balance by Stat3 signaling in the tumor microenvironment. *Cancer Cell.* 15:114–123. http://dx.doi.org/10.1016/j.ccr.2008.12.018

Krueger, G.G., R.G. Langley, C. Leonardi, N. Yeilding, C. Guzzo, Y. Wang, L.T. Dooley, and M. Lebwohl. 2007. A human interleukin-12/23 monoclonal antibody for the treatment of psoriasis. *N. Engl. J. Med.* 356:580–592. http://dx.doi.org/10.1056/NEJMoa062382

Lehmann, J.C., J.J. Listopad, C.U. Rentzsch, F.H. Igney, A. von Bonin, H.H. Hennekes, K. Asadullah, and W.D. Docke. 2007. Dimethylfumarate induces immunosuppression via glutathione depletion and subsequent induction of heme oxygenase 1. *J. Invest. Dermatol.* 127:835–845. http://dx.doi.org/10.1038/sj.jid.5700686

Lin, Q., S. Weis, G. Yang, Y.-H. Weng, R. Helston, K. Rish, A. Smith, J. Bordner, T. Polte, F. Gaunitz, and P.A. Dennery. 2007. Heme oxygenase-1 protein localizes to the nucleus and activates transcription factors important in oxidative stress. *J. Biol. Chem.* 282:20621–20633. http://dx.doi.org/10.1074/jbc.M607954200

Linker, R.A., D.H. Lee, S. Ryan, A.M. van Dam, R. Conrad, P. Bista, W. Zeng, X. Hronowsky, A. Buko, S. Chollate, et al. 2011. Fumaric acid esters exert neuroprotective effects in neuroinflammation via activation of the Nrf2 antioxidant pathway. *Brain.* 134:678–692. http://dx.doi.org/10.1093/brain/awq386

Litjens, N.H., P.H. Nibbering, A.J. Barrois, T.P. Zomerdijk, A.C. Van Den Oudenrijn, K.C. Noz, M. Rademaker, P.H. Van De Meide, J.T. Van Dissel, and B. Thio. 2003. Beneficial effects of fumarate therapy in psoriasis vulgaris patients coincide with downregulation of type 1 cytokines. *Br. J. Dermatol.* 148:444–451. http://dx.doi.org/10.1046/j.1365-2133.2003.05153.x

Litjens, N.H., M. Rademaker, B. Ravensbergen, D. Rea, M.J. van der Plas, B. Thio, A. Walding, J.T. van Dissel, and P.H. Nibbering. 2004. Monomethylfumarate affects polarization of monocyte-derived dendritic cells resulting in down-regulated Th1 lymphocyte responses. *Eur. J. Immunol.* 34:565–575. http://dx.doi.org/10.1002/eji.200324174

Liu, J., X. Guan, T. Tamura, K. Ozato, and X. Ma. 2004. Synergistic activation of interleukin-12 p35 gene transcription by interferon regulatory factor-1 and interferon consensus sequence-binding protein. *J. Biol. Chem.* 279:55609–55617. http://dx.doi.org/10.1074/jbc.M406565200

Liu, W., X. Ouyang, J. Yang, J. Liu, Q. Li, Y. Gu, M. Fukata, T. Lin, J.C. He, M. Abreu, et al. 2009. AP-1 activated by toll-like receptors regulates expression of IL-23 p19. *J. Biol. Chem.* 284:24006–24016. http://dx.doi.org/10.1074/jbc.M109.025528

Loewe, R., W. Holnthoner, M. Gröger, M. Pillinger, F. Gruber, D. Mechtcheriakova, E. Hofer, K. Wolff, and P. Petzelbauer. 2002. Dimethylfumarate inhibits TNF-induced nuclear entry of NF-kappa B/p65 in human endothelial cells. *J. Immunol.* 168:4781–4787.

Lutz, M.B., N. Kukutsch, A.L. Ogilvie, S. Rössner, F. Koch, N. Romani, and G. Schuler. 1999. An advanced culture method for generating large quantities of highly pure dendritic cells from mouse bone marrow. *J. Immunol. Methods.* 223:77–92. http://dx.doi.org/10.1016/S0022-1759(98)00204-X

Mazzoni, A., and D.M. Segal. 2004. Controlling the Toll road to dendritic cell polarization. *J. Leukoc. Biol.* 75:721–730. http://dx.doi.org/10.1189/jlb.1003482

Menges, M., S. Rössner, C. Voigtländer, H. Schindler, N.A. Kukutsch, C. Bogdan, K. Erb, G. Schuler, and M.B. Lutz. 2002. Repetitive injections of dendritic cells matured with tumor necrosis factor alpha induce antigen-specific protection of mice from autoimmunity. *J. Exp. Med.* 195:15–21. http://dx.doi.org/10.1084/jem.20011341

Mise-Omata, S., E. Kuroda, J. Niikura, U. Yamashita, Y. Obata, and T.S. Doi. 2007. A proximal kappaB site in the IL-23 p19 promoter is responsible for RelA- and c-Rel-dependent transcription. *J. Immunol.* 179:6596–6603.

Mrowietz, U., and K. Asadullah. 2005. Dimethylfumarate for psoriasis: more than a dietary curiosity. *Trends Mol. Med.* 11:43–48. http://dx.doi.org/10.1016/j.molmed.2004.11.003

Nair, R.P., K.C. Duffin, C. Helms, J. Ding, P.E. Stuart, D. Goldgar, J.E. Gudjonsson, Y. Li, T. Tejasvi, B.J. Feng, et al. 2009. Genome-wide scan reveals association of psoriasis with IL-23 and NF-kappaB pathways. *Nat. Genet.* 41:199–204. http://dx.doi.org/10.1038/ng.311

Nakahira, K., H.P. Kim, X.H. Geng, A. Nakao, X. Wang, N. Murase, P.F. Drain, X. Wang, M. Sasidhar, E.G. Nabel, et al. 2006. Carbon monoxide differentially inhibits TLR signaling pathways by regulating ROS-induced trafficking of TLRs to lipid rafts. *J. Exp. Med.* 203:2377–2389. http://dx.doi.org/10.1084/jem.20060845

Napolitani, G., A. Rinaldi, F. Bertoni, F. Sallusto, and A. Lanzavecchia. 2005. Selected Toll-like receptor agonist combinations synergistically trigger a T helper type 1-polarizing program in dendritic cells. *Nat. Immunol.* 6:769–776. http://dx.doi.org/10.1038/ni1223

Nestle, F.O., D.H. Kaplan, and J. Barker. 2009. Psoriasis. *N. Engl. J. Med.* 361:496–509. http://dx.doi.org/10.1056/NEJMra0804595

Peterson, J.D., L.A. Herzenberg, K. Vasquez, and C. Waltenbaugh. 1998. Glutathione levels in antigen-presenting cells modulate Th1 versus Th2 response patterns. *Proc. Natl. Acad. Sci. USA.* 95:3071–3076. http://dx.doi.org/10.1073/pnas.95.6.3071

Polman, C.H., P.W. O'Connor, E. Havrdova, M. Hutchinson, L. Kappos, D.H. Miller, J.T. Phillips, F.D. Lublin, G. Giovannoni, A. Wajgt, et al. 2006. A randomized, placebo-controlled trial of natalizumab for relapsing multiple sclerosis. *N. Engl. J. Med.* 354:899–910. http://dx.doi.org/10.1056/NEJMoa044397

Racke, M.K., A. Bonomo, D.E. Scott, B. Cannella, A. Levine, C.S. Raine, E.M. Shevach, and M. Röcken. 1994. Cytokine-induced immune deviation as a therapy for inflammatory autoimmune disease. *J. Exp. Med.* 180:1961–1966. http://dx.doi.org/10.1084/jem.180.5.1961

Rothfuss, O., H. Fischer, T. Hasegawa, M. Maisel, P. Leitner, F. Miesel, M. Sharma, A. Bornemann, D. Berg, T. Gasser, and N. Patenge. 2009. Parkin protects mitochondrial genome integrity and supports mitochondrial DNA repair. *Hum. Mol. Genet.* 18:3832–3850. http://dx.doi.org/10.1093/hmg/ddp327

Schilling, S., S. Goelz, R. Linker, F. Luehder, and R. Gold. 2006. Fumaric acid esters are effective in chronic experimental autoimmune encephalomyelitis and suppress macrophage infiltration. *Clin. Exp. Immunol.* 145:101–107. http://dx.doi.org/10.1111/j.1365-2249.2006.03094.x

Schuler, G., B. Schuler-Thurner, and R.M. Steinman. 2003. The use of dendritic cells in cancer immunotherapy. *Curr. Opin. Immunol.* 15:138–147. http://dx.doi.org/10.1016/S0952-7915(03)00015-3

Segal, B.M., C.S. Constantinescu, A. Raychaudhuri, L. Kim, R. Fidelus-Gort, and L.H. Kasper. 2008. Repeated subcutaneous injections of IL12/23 p40 neutralising antibody, ustekinumab, in patients with relapsing-remitting multiple sclerosis: a phase II, double-blind, placebo-controlled, randomised, dose-ranging study. *Lancet Neurol.* 7:796–804. http://dx.doi.org/10.1016/S1474-4422(08)70173-X

Tzima, S., P. Victoratos, K. Kranidioti, M. Alexiou, and G. Kollias. 2009. Myeloid heme oxygenase–1 regulates innate immunity and autoimmunity by modulating IFN-β production. *J. Exp. Med.* 206:1167–1179. http://dx.doi.org/10.1084/jem.20081582

Weber, M.S., T. Prod'homme, S. Youssef, S.E. Dunn, C.D. Rundle, L. Lee, J.C. Patarroyo, O. Stüve, R.A. Sobel, L. Steinman, and S.S. Zamvil. 2007. Type II monocytes modulate T cell-mediated central nervous system autoimmune disease. *Nat. Med.* 13:935–943. http://dx.doi.org/10.1038/nm1620

Zhu, C., K. Rao, H. Xiong, K. Gagnidze, F. Li, C. Horvath, and S. Plevy. 2003. Activation of the murine interleukin-12 p40 promoter by functional interactions between NFAT and ICSBP. *J. Biol. Chem.* 278:39372–39382. http://dx.doi.org/10.1074/jbc.M306441200